Optimization of an Industrial Semibatch Nylon 6 Reactor

R. SAREEN, M. R. KULKARNI, and S. K. GUPTA*

Department of Chemical Engineering, Indian Institute of Technology, 208016 Kanpur, India

SYNOPSIS

An industrial semibatch nylon 6 reactor has been optimized using a one-variable (at a time) search technique. The vapor release rate from the reactor and the final monomer conversion have been constrained to lie very close to the values currently present. The degree of polymerization of the product is, similarly, constrained to lie at a value of 152. The optimal pressure histories for two values of the jacket fluid temperature, T_j, have been evaluated using two objective functions, I_1 and I_3, namely, the total reaction time ($I_1 = t_f$) and the concentration of the cyclic dimer ($I_3 = [C_2]_f$) in the product. It is observed that as T_j is increased from 270 to 280°C, I_1 improves while I_3 worsens simultaneously. This suggests that these two optimal points lie on the Pareto set for the two-objective function problem.

INTRODUCTION

A considerable amount of research has been reported on the optimization of polymerization reactors in recent years. This includes the computation of optimal temperature or initiator-addition histories for batch or semibatch free radical[1-3] or step growth[4-8] polymerization reactors using Pontryagin's maximum (minimum) principle.[1] These studies have been carried out under a variety of constraints, using different single-objective functions as well as multiple-objective functions.[3,8] Not much work has been reported on the application of these techniques to *industrial* polymerization reactors. This study is an attempt along this direction. In this work we obtain optimal pressure histories for a semibatch nylon 6 reactor in an industrial setting. Theoretical results only are presented since actual data indicating the improvement of reactor performance cannot be furnished due to proprietary reasons. In this industrial reactor, vaporization of ϵ-caprolactam (monomer) and water can be manipulated using a control valve. This reactor has been simulated by our group recently[9-11] and the model so developed is used for optimization. It has been shown that a substantial improvement is possible in the performance of the reactor by changing the pressure history.

The industrial reactor studied is shown schematically in Figure 1. The reactor is a jacketed vessel with a low-speed anchor or ribbon agitator used for mixing the highly viscous reaction mass. The reaction mass is heated by condensing vapors in the jacket. Pressure is manipulated to conform to a desired history by a control valve which allows the vapor mixture of nitrogen, monomer, and water to pass to a condenser. The pressure history in the reactor used presently [termed as reference (ref)], is shown in Figure 2 (curve r), in terms of the following dimensionless variables:

$$\Pi \equiv (p - p_0)/(p_{\max,\mathrm{ref}} - p_0) \tag{1a}$$

$$\tau \equiv t/t_{f,\mathrm{ref}} \tag{1b}$$

where the values of the maximum pressure, $p_{\max,\mathrm{ref}}$, and total reaction time, $t_{f,\mathrm{ref}}$, are not being mentioned for proprietary reasons. Actual data points for the industrial reactor are compared with the solid curve in Ref. 11 for the feed water concentration, $[W]_0$, of 3.45% (by weight). The present pressure history can be described in terms of five zones:

1. In zone 1, the valve is closed and the pressure in the reactor builds up to the value $p_{\max,\mathrm{ref}}$.

* To whom correspondence should be addressed.

Journal of Applied Polymer Science, Vol. 57, 209–218 (1995)
 CCC 0021-8995/95/020209-10

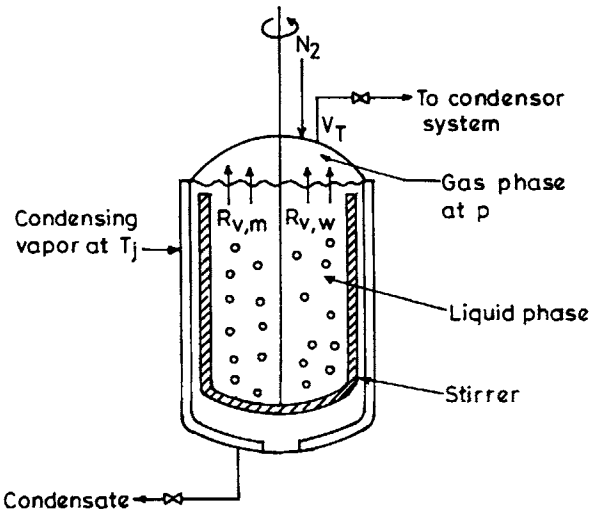

Figure 1 Schematic representation of the industrial semibatch nylon 6 reactor.

2. In zone 2, p is kept at $p_{max,ref}$ for a time period $t_{c,ref}$, using vapor release through the valve.
3. In zones 3, 4, and 5, p decreases linearly with time. The slopes of the p vs. t graph differ in these three zones. The value of p at $t = t_{f,ref}$ is slightly above atmospheric (1.04 atm). These are achieved by the action of the control valve.

The jacket temperature, T_j, is kept constant throughout the reaction. This heats up the reaction mass in the initial period. The simulated temperature history in the industrial reactor and the experimental points are available in Ref. 11.

A few preliminary simulation runs were conducted using the computer program developed in Ref. 11, and it was concluded that the pressure history could easily be modified and simplified for use in optimization. In the simplified pressure history, p builds up to a maximum value, p_{max}, in the initial period, when the valve is closed. The pressure is then kept constant at p_{max} for a time period t_c, after which p decreases linearly with time with a slope S ($=dp/dt$) till it reaches $p = 1.04$ atm. Finally, p is maintained at this value till $t = t_f$, where t_f is the total reaction time. The values of p_{max}, t_c, and t_f need not be the same as $p_{max,ref}$, $t_{c,ref}$, and $t_{f,ref}$ used in the industrial reactor currently (prior to optimization). Thus, the simplified pressure history can be completely described by four parameters, viz., p_{max}, t_c, S, and t_f. Since t_f will be decided by the attainment of the desired degree of polymerization, $\mu_n(t = t_f) = \mu_{n,d}$, this leaves only three parameters (p_{max}, t_c, and S) which need to be optimized. The problem, thus, is to choose p_{max}, t_c, and S so as to optimize one or more objective functions, subject to the attainment of a fixed value of the number-average chain length of the final product. Such an optimization problem in which the shape of the pressure history is fixed (similar to what is currently being used), is far simpler than the problem in which the entire pressure history, $p(t)$, is to be optimized using Pontryagin's minimum principle.

FORMULATION

We have focused on the following objective functions in this study:

1. Minimization of the dimensionless reaction time (min $I_1 \equiv t_f/t_{f,ref}$): the reaction time, t_f, is determined by the time required for the DP (degree of polymerization = μ_n) to reach a desired value, $\mu_{n,d}$. Minimization of $t_f/t_{f,ref}$ would lead to higher production capacity.
2. Maximization of the final monomer conversion (max $I_2 \equiv \text{conv}_f/\text{conv}_{f,ref}$), where conv is defined by

$$\text{conv} = 1.0 - (F[C_1] + \zeta_1)/(F_0[C_1]_0) \quad (2)$$

The conversion reflects the amount of monomer entrapped in the product, which needs to be removed and so represents a loss. The

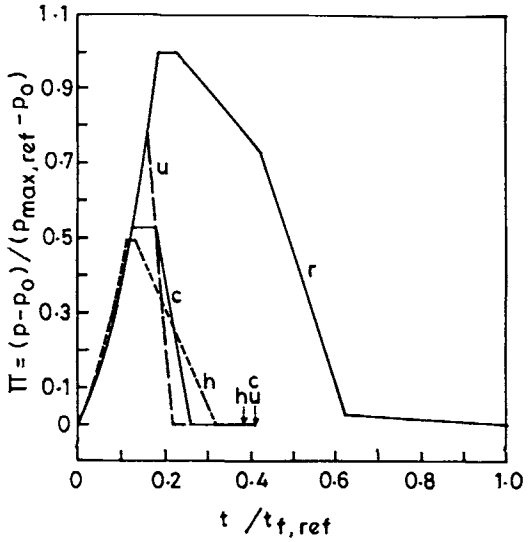

Figure 2 Dimensionless pressure histories for the semibatch reactor. Curves (r): reference value, (c): I_4-constrained optimal, (u): unconstrained optimal; with T_j = 270°C. Curve h indicates constrained optimal with T_j = 280°C.

definition of conversion in Eq. (2) incorporates the cumulative evaporation of monomer in the reactor, represented by the term ζ_1 (alternate definitions of conv can be used too).

3. Minimization of the undesirable cyclic dimer in the final product (min $I_3 = [C_2]_f/[C_2]_{f,\text{ref}}$): though the amount of cyclic dimer formed is below about 2–3% (by weight), this causes problems in polymer processing and needs to be extracted using an energy-intensive and expensive hot water leaching process.

These three objective functions are not necessarily compatible and need to be studied carefully. Multiobjective optimization using subjective judgment was used to decide the best operating conditions (values of $p_{\max}$, t_c, and S for a given value of T_j and feed). Alternatively, we could have used a single-objective function involving a weighted sum of the three individual objective functions. The latter was not selected since the choice of weightage factors introduces as much subjectivity as present in choosing the optimal solution using judgment.

The kinetic scheme, rate constants,[12–14] and the mass balance and moment equations used are described in detail in Ref. 11 and are not repeated here for the sake of brevity. The stiff[15] ordinary differential equations are integrated using the D02EJF subroutine of the NAG library with an error tolerance of 10^{-6}. The change in viscosity of the reaction mixture and its effect on the mass transfer rates have been incorporated using correlations for the viscosity and the activity coefficients of water and ε-caprolactam. These correlations have been developed by curve-fitting one set of industrial data, and have been found to be quite satisfactory for other operating conditions.

The computer code finally developed[11] predicts several macro as well as micro properties of the polymer product. These include the number-average molecular weight or degree of polymerization, the polydispersity index (PDI), water extractibles, cyclic dimer concentration, monomer conversion, etc. In addition, reactor characteristics like heat and mass transfer aspects, temperature, T, of the reaction mass, vapor discharge rate, V_t, at any time, etc., are also predicted. This computer code is coupled with an optimization code which performs a single-parameter search[16] in the three parameter ($p_{\max}$, t_c, and S) space at any stage. The three objective functions, I_1, I_2, and I_3, are predicted for every choice of the parameter selected for search and a decision is made as to the best value by looking at the plots of the three objective functions. Search over all three parameters, one at a time, completes one cycle of optimization (comprising of three stages).

While performing the one-parameter search, the three parameters were constrained to lie within certain limiting values. These were selected as

$$\begin{aligned} 0.4 &\le p_{\max}/p_{\max,\text{ref}} \le 1.0 \\ -9 &\le S \le -1 \\ 0 &\le t_c/t_{f,\text{ref}} \le 0.14 \end{aligned} \tag{3}$$

RESULTS AND DISCUSSION

The reference results were first generated using the simulation code developed by Wajge et al.[11] The reference run represents operating conditions actually used in the industrial reactor prior to optimization. It corresponds to the following operating conditions[11]:

$$\begin{aligned} [C_1]_0 &= 8.5442 \text{ mol/kg} \\ [W]_0 &= 1.91667 \text{ mol/kg (3.45\% by weight)} \\ T_0 &= 90°\text{C} \\ T_j &= 270°\text{C} \\ p_0 &= 101.3 \text{ kPa} \end{aligned} \tag{4}$$

The values of $p_{\max,\text{ref}}$, $t_{f,\text{ref}}$, F, $[N^v]_0$, D_r, d_s, n, and V_g (see Nomenclature) are not reported to ensure confidentiality. These results were found to match those reported earlier[11] and lend confidence on the correctness of the simulation code used.

Optimization by single-parameter search was then carried out for $[W]_0 = 3.45\%$ and $\mu_{n,d} = 152$. The first parameter explored (stage 1) in the first cycle was $p_{\max}/p_{\max,\text{ref}}$. The values of the other two parameters were kept constant during this search at $S = -5$, and $t_c = 0$. The results are shown in Figures 3–6. A distinct minima in I_1 is observed at $p_{\max}/p_{\max,\text{ref}} = 0.7714$, but the final conversion obtained at this value of $p_{\max}/p_{\max,\text{ref}}$ is low. $p_{\max}/p_{\max,\text{ref}} = 0.8286$ appears to be the best value since this takes the monomer conversion to the asymptotic level, while not worsening I_1 too much. The value of I_3 at this point (indicated by arrow u in Figs. 3–6) is also reasonably low. At this point it is interesting to observe the effect of varying $p_{\max}/p_{\max,\text{ref}}$ on $V_{t,\max}$, the maximum value of the vapor release rate (mole vapor released from valve/hour). This is shown in Figure 6 using the industrial (reference) value $V_{t,\max,\text{ref}}$ to nondimensionalize this variable. It is observed that the maximum vapor release ($I_4 \equiv V_{t,\max}/V_{t,\max,\text{ref}}$) is

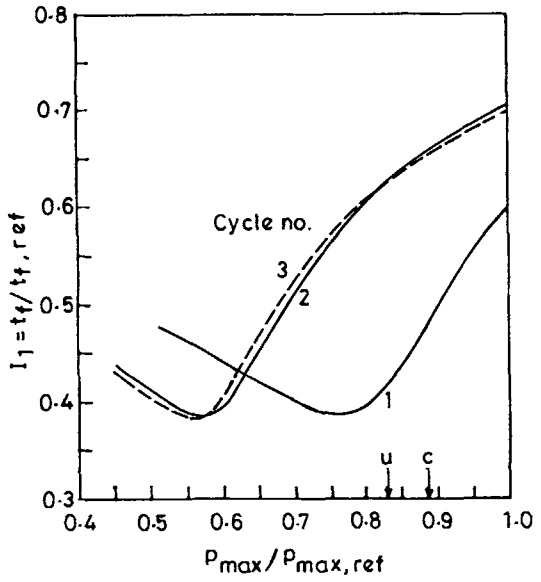

Figure 3 I_1 vs. $p_{max}/p_{max,ref}$ for $[W]_0 = 3.45\%$, $\mu_{n,d} = 152$, $T_j = 270°C$. Cycle numbers are indicated. Values of $|S|$ and $t_c/t_{f,ref}$ for each curve are given in Table I. Arrows represent optimal choices for cycle No. 1.

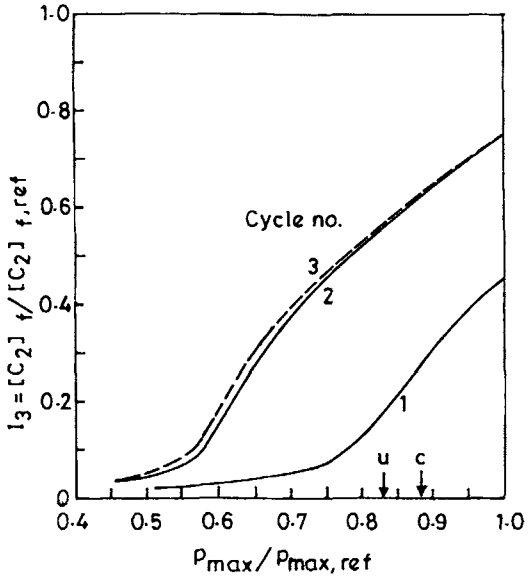

Figure 5 I_3 vs. $p_{max}/p_{max,ref}$ for $[W]_0 = 3.45\%$, $\mu_{n,d} = 152$, $T_j = 270°C$. Notation same as in Figure 3.

quite high, and it is likely that the control valve installed in the reactor may not be able to release vapor at such high rates. It was, therefore, decided to make $V_{t,max}/V_{t,max,ref}$ as close to (or below) unity as possible (this is really a constraint being put on optimization). Figure 6 shows that $p_{max}/p_{max,ref} = 0.8857$ is a better operating point since it leads to lower values of I_4 while not worsening I_1 and I_3 too much. This point is finally selected as the best in this stage, and is indicated by the arrow c (for constrained optimization) in Figures 3–6. The use of all four objective functions and evaluations of alternatives using mental judgment is well illustrated from this discussion.

After the search on $p_{max}/p_{max,ref}$, stage 2 of the first cycle starts. We use $p_{max}/p_{max,ref} = 0.8857$ and $t_c/t_{f,ref} = 0$, and vary the parameter, S. Figures 7–10

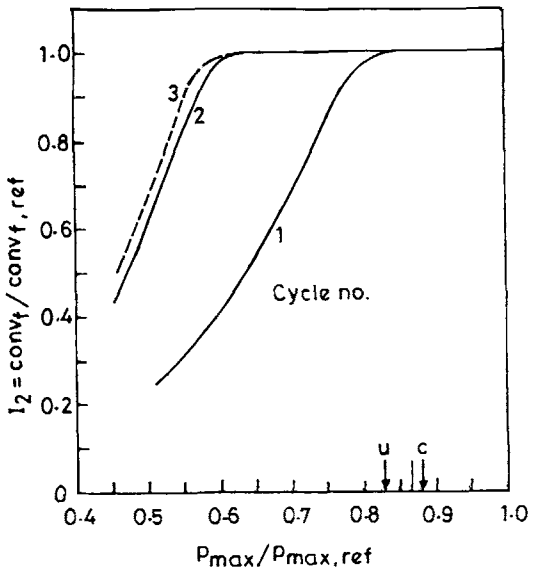

Figure 4 I_2 vs. $p_{max}/p_{max,ref}$ for $[W]_0 = 3.45\%$, $\mu_{n,d} = 152$, $T_j = 270°C$. Notation same as in Figure 3.

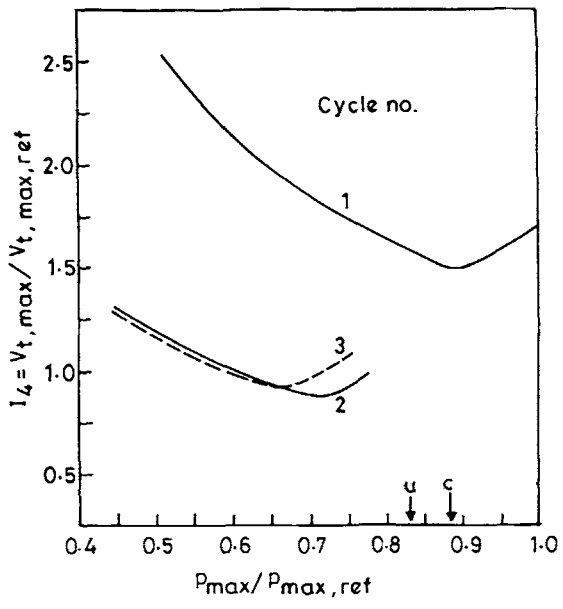

Figure 6 I_4 vs. $p_{max}/p_{max,ref}$ for $[W]_0 = 3.45\%$, $\mu_{n,d} = 152$, $T_j = 270°C$. Notation same as in Figure 3.

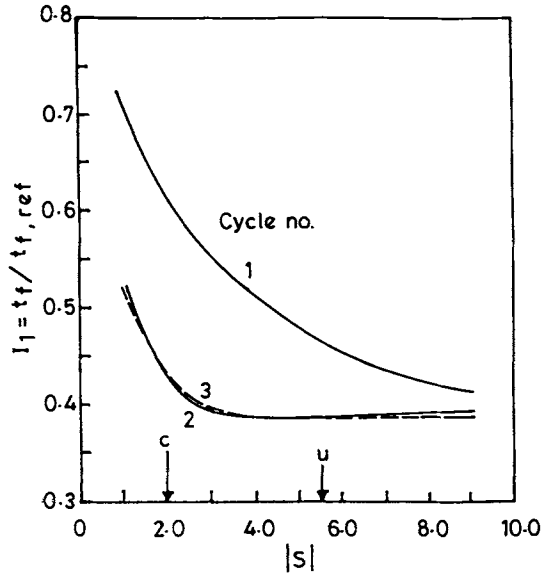

Figure 7 I_1 vs. $|S|$ for $[W]_0$ = 3.45%, $\mu_{n,d}$ = 152, T_j = 270°C. Cycle numbers are indicated. Values of $p_{max}/p_{max,ref}$ and $t_c/t_{f,ref}$ for each curve are given in Table I. Arrows represent optimal choices for cycle No. 1.

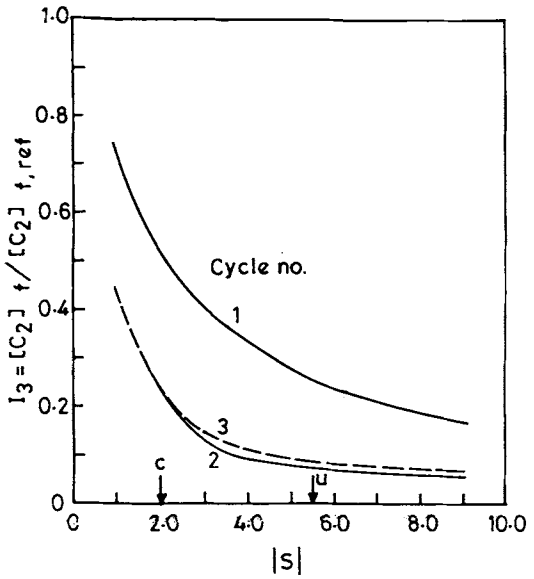

Figure 9 I_3 vs. $|S|$ for $[W]_0$ = 3.45%, $\mu_{n,d}$ = 152, T_j = 270°C. Notation same as in Figure 7.

show the results. The value of I_2 is close to unity for $0 < |S| < 10$. A value of S of -2.0 is selected as the best. This corresponds to $V_{t,max}/V_{t,max,ref}$ of about 1.0. Change of $|S|$ from 5 to 2 forces the constraint (I_4) to be satisfied, while not worsening I_1 and I_3 too much (I_2 is unaffected). Once again, it is seen that I_4 decides the optimal value of $|S|$ since I_1 and I_3 are still below 1.0. After this step, we search for the third parameter, $t_c/t_{f,ref}$, keeping $p_{max}/p_{max,ref}$ = 0.8857 and $S = -2$. The results are shown in Figures 11–14. We get $I_2 = conv_f/conv_{f,ref} \approx 1$ for $0 < t_c/t_{f,ref} < 0.14$. Once again, since I_1 and I_3 are less than 1, the constraint, I_4, decides the best value of the parameter being studied, and $t_c/t_{f,ref}$ is chosen as 0.034. This makes $I_4 \approx 1$. At the end of the first cycle, thus, we have $p_{max}/p_{max,ref}$ = 0.8857, $|S|$ = 2 and $t_c/t_{f,ref}$ = 0.034. The single variable search is continued over more cycles until the results do not change much.

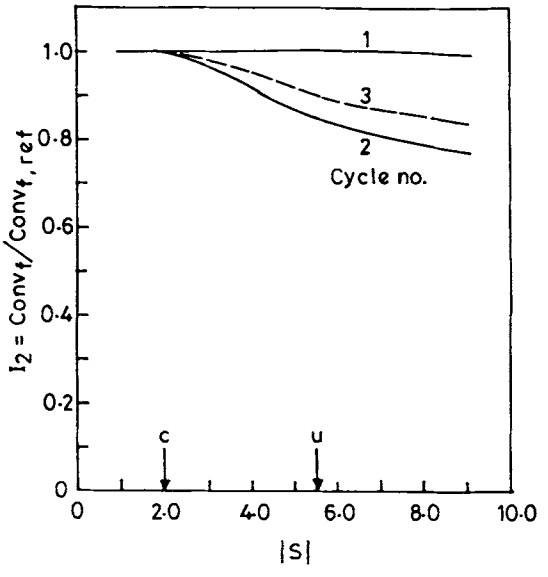

Figure 8 I_2 vs. $|S|$ for $[W]_0$ = 3.45%, $\mu_{n,d}$ = 152, T_j = 270°C. Notation same as in Figure 7.

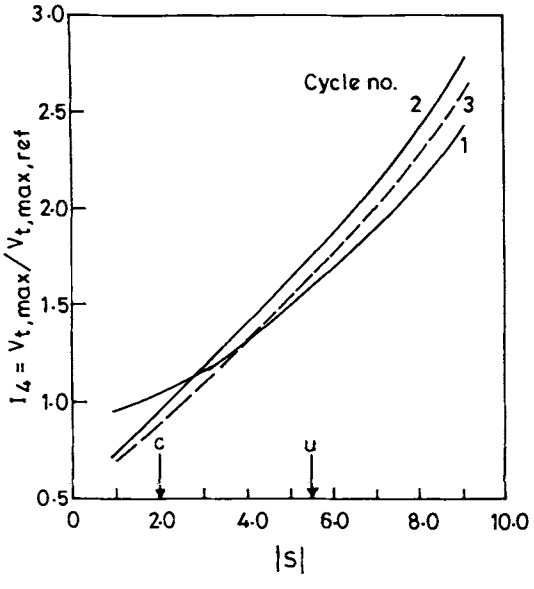

Figure 10 I_4 vs. $|S|$ for $[W]_0$ = 3.45%, $\mu_{n,d}$ = 152, T_j = 270°C. Notation same as in Figure 7.

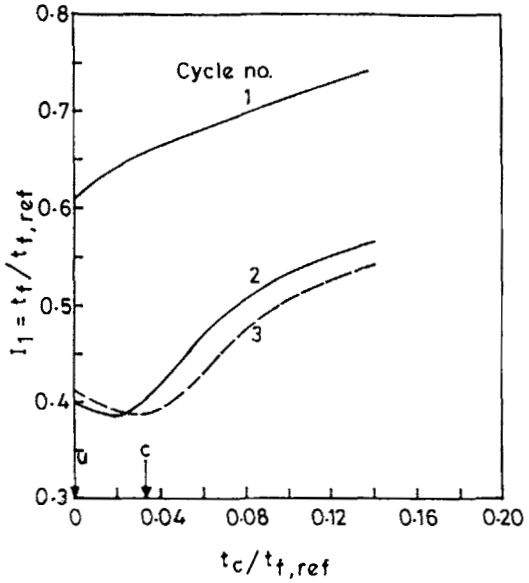

Figure 11 I_1 vs. $t_c/t_{f,ref}$ for $[W]_0 = 3.45\%$, $\mu_{n,d} = 152$, $T_j = 270°C$. Cycle numbers are indicated. Values of $p_{max}/p_{max,ref}$ and $|S|$ for each curve are given in Table I. Arrows indicate optimal choices for the constrained (c) and unconstrained (u) cases for cycle No. 1.

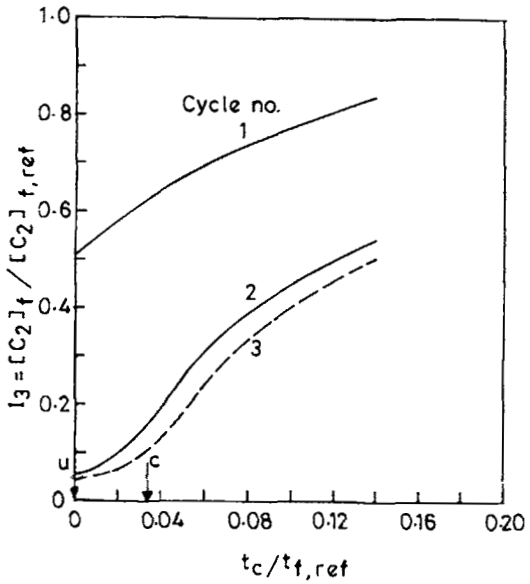

Figure 13 I_3 vs. $t_c/t_{f,ref}$ for $[W]_0 = 3.45\%$, $\mu_{n,d} = 152$, $T_j = 270°C$. Notation same as in Figure 11.

Detailed results for three cycles are shown in Table I, while corresponding plots for $I_1 - I_4$ for the three cycles are also shown in Figures 3–14. The sequence of decisions made stage by stage (as shown in Table I) can easily be deduced from these diagrams. The final dimensionless pressure history for the optimal conditions is shown as curve c (incorporating the I_4 constraint) in Figure 2.

A similar search was carried out for the unconstrained case in which I_4 was not considered to be important, i.e., the control valve can handle larger vapor release rates than in the present reactor. The unconstrained optimum in the first stage of the first cycle has been discussed earlier, and is shown by the arrow marked u in Figures 3–6. The detailed

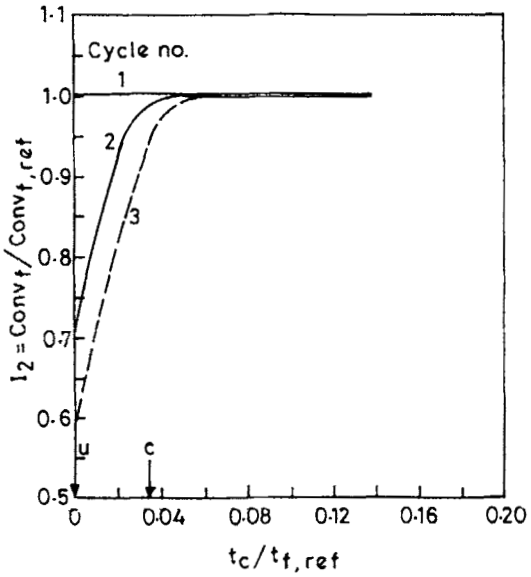

Figure 12 I_2 vs. $t_c/t_{f,ref}$ for $[W]_0 = 3.45\%$, $\mu_{n,d} = 152$, $T_j = 270°C$. Notation same as in Figure 11.

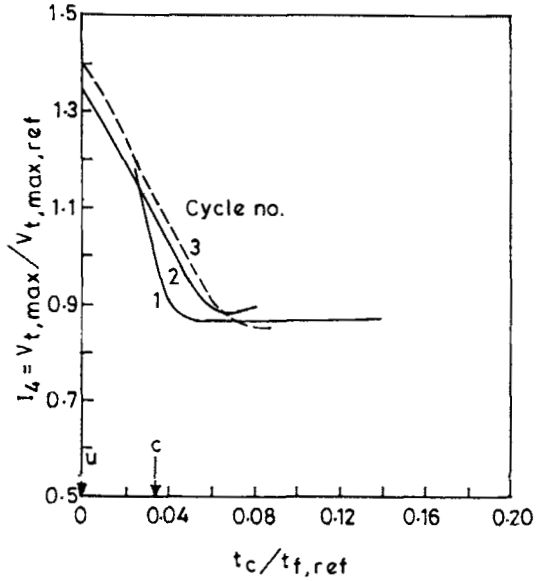

Figure 14 I_4 vs. $t_c/t_{f,ref}$ for $[W]_0 = 3.45\%$, $\mu_{n,d} = 152$, $T_j = 270°C$. Notation same as in Figure 11.

Table I Results of Constrained Multiobjective Optimization[a]

T_j	$p_{max}/p_{max,ref}$	$\|S\|$	$t_c/t_{f,ref}$	I_1	I_2	I_3	I_4
270°	First cycle						
	0.8857	5	0	0.4748	1.0037	0.2776	1.4945[b]
	0.8857	2	0	0.6083	1.0022	0.5126	1.0459[b]
	0.8857	2	0.034	0.6576	1.0023	0.6224	0.9669[b]
	Second cycle						
	0.6286	2	0.034	0.4268	0.9977[b]	0.2276	0.9578
	0.6286	2.5	0.034	0.4014	0.9903[b]	0.1626	1.0697
	0.6286	2.5	0.05	0.4414	0.9995[b]	0.2545	0.9435
	Third cycle						
	0.6	2.5	0.05	0.4074	0.9935[b]	0.1807	0.9852
	0.6	2.5	0.05	0.4074	0.9935[b]	0.1807	0.9852
	0.6	2.5	0.05	0.4074	0.9935[b]	0.1807	0.9852
280°C	Third cycle	(final)					
	0.5714	1.0	0.0181	0.3841	0.9886	0.2581	0.9850

[a] Values at the end of each stage in a cycle are included for T_j 270°C.
[b] Indicates the deciding objective function/constraint.

results for this case are shown in Table II. The optimum pressure history ($p_{max}/p_{max,ref} = 0.8286$, $|S| = 5.5$, $t_c/t_{f,ref} = 0$) is shown by curve u in Figure 2. It is interesting to observe that the unconstrained case gives almost the same product in about the same reaction time, as the constrained case. The value of I_4 for the optimal pressure history in the unconstrained case comes out as 1.6997, which is much larger than the value of 0.9852 obtained for the constrained optimization.

The various characteristics of the polymer and of the reactor operation are shown in Figures 15–20. Figure 15 shows the dimensionless temperature history for the two optimal conditions (c and u) as well as for the reference run. The experimental data on the industrial reactor (prior to optimization) is also shown.[11] The two optimal temperature histories deviate from the current one at $\tau \approx 0.2$ because of the considerable variation of the pressure history around that time (which leads to substantially different vapor release histories, having its influence on the temperature through latent heat effects). Figure 16 shows the variation of the monomer conversion histories with τ. It is interesting to observe that the conversion rises less sharply than in the reference case. This is associated with the lower temperatures in the optimal cases. Figure 17 shows how the degree of polymerization increases with τ for the optimal as well as the reference runs. In the reference run, two distinct regimes are observed where DP increases, the first being associated with the polyaddition reaction while the second with the polycondensation reaction.[11] There is a short plateau inbetween these. Figure 17 shows that this plateau does not exist for the two optimal histories because of the early and rapid pressure decrease, and the DP increases rapidly at an almost constant rate to the desired value of 152. It may be mentioned here that the value of μ_n almost approaches its asymptotic value at $t_{f,ref}$ for the reference case. This is not so

Table II Results of Unconstrained Multiobjective Optimization[a]

$p_{max}/p_{max,ref}$	$\|S\|$	$t_c/t_{f,ref}$	I_1	I_2	I_3	I_4
First cycle						
0.8286	5	0	0.4142	0.9949[b]	0.1763	1.5900
0.8286	5.5	0	0.4047	0.9897[b]	0.1560[b]	1.6996
0.8286	5.5	0	0.4047[b]	0.9897	0.1560[b]	1.6996
Second cycle						
0.8286	5.5	0	0.4047	0.9897[b]	0.1560	1.6996

[a] Value at the end of each stage in a cycle are included. T_j = 270°C.
[b] Indicates the deciding objective function/constraint.

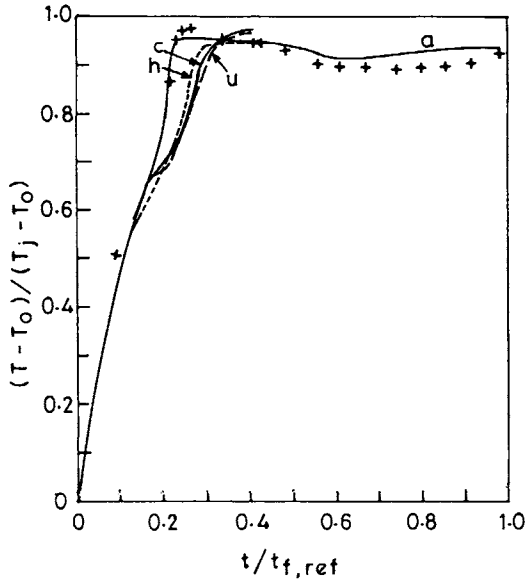

Figure 15 Variation of the dimensionless temperature with dimensionless time for the reference (*a*), constrained (*c*), and unconstrained (*u*) runs for T_j = 270°C. Curve *h* is for the constrained optimal for T_j = 280°C. Industrial points for the reference case[11] also shown. $[W]_0$ = 3.45%, $\mu_{n,d}$ = 152.

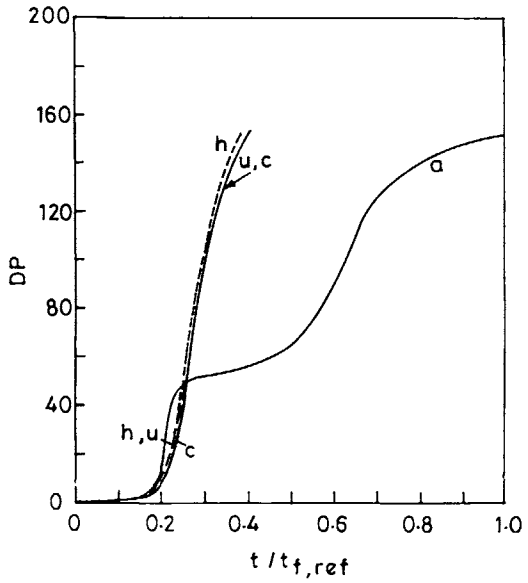

Figure 17 Variation of the degree of polymerization with dimensionless time for the reference (*a*), constrained (*c*), and unconstrained (*u*) runs for T_j = 270°C. Curve *h* is for the constrained optimal for T_j = 280°C. $[W]_0$ = 3.45%, $\mu_{n,d}$ = 152.

for the two optimal runs and suggests the need for excellent control of the reactor so that the value of μ_n of the product does not overshoot the desired value. Since the level of expertise available these days in the area of control is quite good, this should pose no major problem.

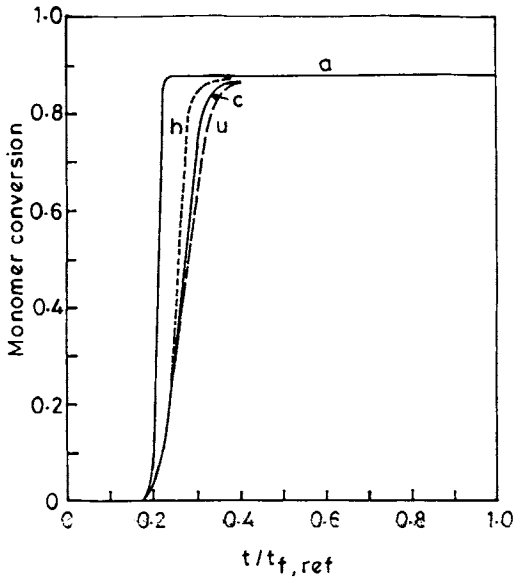

Figure 16 Variation of monomer conversion with dimensionless time for the reference (*a*), constrained (*c*), and unconstrained (*u*) runs for T_j = 270°C. Curve *h* is for the constrained optimal for T_j = 280°C. $[W]_0$ = 3.45%, $\mu_{n,d}$ = 152.

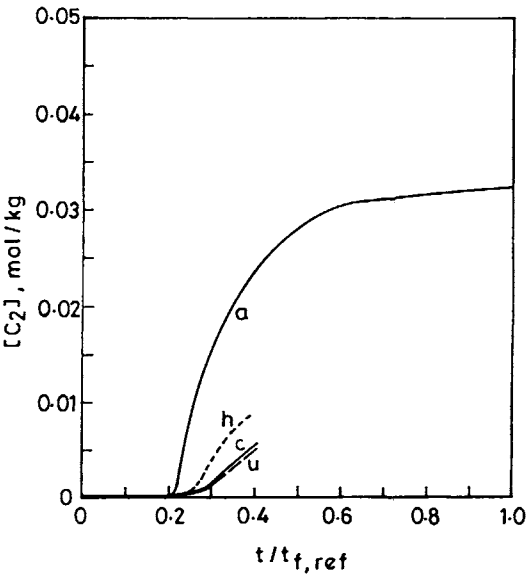

Figure 18 Variation of the cyclic dimer concentration with dimensionless time for the reference (*a*), constrained (*c*), and unconstrained (*u*) runs for T_j = 270°C. Curve *h* is for the constrained optimal for T_j = 280°C. $[W]_0$ = 3.45%, $\mu_{n,d}$ = 152.

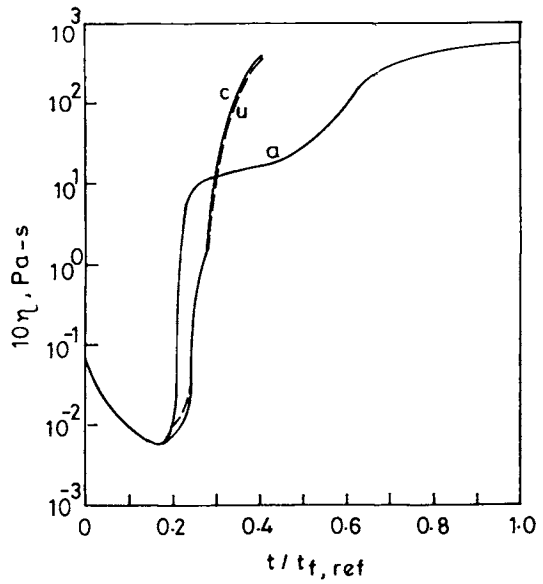

Figure 19 Variation of the viscosity of the reaction mixture with dimensionless time for the reference (*a*), constrained (*c*), and unconstrained (*u*) runs. $[W]_0 = 3.45\%$, $\mu_{n,d} = 152$, $T_j = 270°C$.

The increase of the undesirable cyclic dimer concentration, $[C_2]$, is shown in Figure 18. It is seen that the dimer concentration remains negligible upto τ of about 0.2. After this it rises considerably for the reference run but only very slightly for the two optimal runs. It must be emphasized that the low values of $[C_2]_f$ for optimal runs may increase further during postpolymerization processes, since equilibrium is not attained for the reactions involving the cycle dimer.

Agitation of the reaction mass is strongly dependent on its viscosity, and hence the variation of viscosity with time needs to be studied. Figure 19 shows that the viscosity of the reaction mass for the optimal runs increases rapidly to almost the same final value as for the reference run. This is associated with the faster increase in the average molecular weight, as shown for DP in Figure 17.

Figure 20 shows the vapor release rate through the valve for the reference and optimal runs. Two distinct maxima in the vapor flow rates are observed for the reference case and the unconstrained optimal case, but not for the constrained case. The early maximum corresponds to the opening of the valve for the first time, while the later one is associated with the rapid fall of the pressure. It is interesting to note that even though the final product characteristics for the two optimal runs are not too different, the pressure histories required and the associated vapor release rates differ significantly.

We also carried out optimization for a slightly higher jacket temperature ($T_j = 280°C$), with the other parameters unchanged. The optimal results are shown in Table I. The final values of the two constraints, $V_{t,\max}/V_{t,\max,\text{ref}}$ ($\equiv I_4$) and $\text{conv}_f/\text{conv}_{f,\text{ref}}$ ($\equiv I_2$), have been kept very close to the values corresponding to the $T_j = 270°C$ case. It is interesting to observe that for higher jacket temperatures, the optimal value of I_1 ($\equiv t_f/t_{f,\text{ref}}$) is better while that of I_3 ($\equiv [C_2]_f/[C_2]_{f,\text{ref}}$) is worse than for the $T_j = 270°C$ case. Which of these two jacket temperatures is to be used can now be decided upon by a "decision maker,"[8,17] depending on the emphasis he puts on the two objective functions. In fact, the optimal results for the two jacket temperatures studied herein strongly suggest that a more rigorous multiobjective optimization study be carried out, and Pareto optimal sets be generated (such a study is being pursued now by our group). The pressure, temperature, conversion, DP, and $[C_2]$ histories for the optimal run for $T_j = 280°C$ have been included in Figures 2 and 15–18, respectively. The higher buildup of C_2 and the earlier rise of DP to $\mu_{n,d}$ as compared to the $T_j = 270°C$ case, are observed in Figures 18 and 17, respectively.

CONCLUSIONS

Two multiobjective optimal solutions for an industrial semibatch nylon 6 reactor have been obtained.

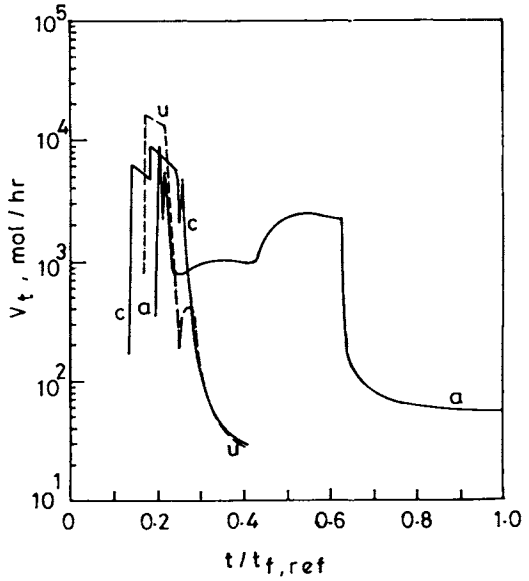

Figure 20 Variation of vapor release rate, V_t, through the control valve with dimensionless time for the reference (*a*), constrained (*c*), and unconstrained (*u*) runs. $[W]_0 = 3.45\%$, $\mu_{n,d} = 152$, $T_j = 270°C$.

Considerable improvement in the reactor operation has been predicted. Lower pressures and faster vapor releases are required to achieve such operation. However, better control of the reactor is necessary since the product is not a near-equilibrium material.

NOMENCLATURE

$[C_i]$	concentration of caprolactam (i = 1) and cyclic dimer (i = 2) in the liquid phase (mol/kg mixture)
conv	conversion [Eq. (2)]
d_s	diameter of stirrer (m)
DP	degree of polymerization
D_r	diameter of reactor (m)
F	mass of liquid in reactor at time t (kg)
I	objective function (dimensionless)
n	rate of rotation of stirrer (rpm)
$[N^v]$	concentration of nitrogen in vapor phase (mol/m^3)
p	total pressure (kPa)
S	slope of p vs. t graph in the third stage (atm/h)
t	time (h)
t_c	time for which pressure remains constant at p_{max} (h)
t_f	total reaction time (h)
T	temperature (K)
V_g	volume of vapor space (m^3)
V_t	rate of vapor release from reactor (mol/h)
$[W]$	water concentration in liquid (mol/kg mixture)

Greek Letters

μ_n	number–average chain length = DP
$\mu_{n,d}$	desired value of μ_n in the final product
η	viscosity of liquid mixture (Pa s or poise; 1 poise = 10^{-1} Pa s)
Π	dimensionless pressure [Eq. (1)]
τ	dimensionless time [Eq. (1)]
ζ_1	total mole of monomer vaporized till time t (mol)

Subscripts/Superscripts

f	final value (product)
j	jacket
max	maximum value
0	feed conditions
ref	reference value (industrial value before optimization)

REFERENCES

1. J. N. Farber, in *Handbook of Polymer Science and Technology,* N. P. Cheremisinoff, Ed., Vol. 1, Marcel Dekker, New York, 1989, p. 429.
2. B. M. Louie and D. S. Soong, *J. Appl. Polym. Sci.,* **30,** 3707 (1985).
3. A. Tsoukas, M. Tirrell, and G. Stephanopoulos, *Chem. Eng. Sci.,* **37,** 1785 (1982).
4. S. K. Gupta, B. S. Damania, and A. Kumar, *J. Appl. Polym. Sci.,* **29,** 2177 (1984).
5. A. Ramagopal, A. Kumar, and S. K. Gupta, *J. Appl. Polym. Sci.,* **28,** 2261 (1983).
6. A. K. Ray and S. K. Gupta, *Polym. Eng. Sci.,* **26,** 1033 (1986).
7. D. Srivastava and S. K. Gupta, *Polym. Eng. Sci.,* **31,** 596 (1991).
8. R. M. Wajge and S. K. Gupta, *Polym. Eng. Sci.,* **34,** 1161 (1994).
9. A. Gupta, S. K. Gupta, K. S. Gandhi, B. V. Ankleswaria, M. H. Mehta, M. R. Padh, and A. V. Soni, in *Recent Trends in Chemical Reaction Engineering,* B. D. Kulkarni, R. A. Mashelkar, and M. M. Sharma, Eds., Wiley Eastern, New Delhi, 1987, p. 281.
10. A. Gupta, S. K. Gupta, K. S. Gandhi, M. H. Mehta, M. R. Padh, A. V. Soni, and B. V. Ankleswaria, *Chem. Eng. Commun.,* **113,** 63 (1992).
11. R. M. Wajge, S. S. Rao, and S. K. Gupta, *Polymer,* **35,** 3722 (1994).
12. H. K. Reimchuessel, *J. Polym. Sci., Macromol. Rev.,* **12,** 65 (1977).
13. K. Tai and T. Tagawa, *Ind. Eng. Chem., Prod. Res. Dev.,* **22,** 192 (1983).
14. S. K. Gupta and A. Kumar, *Reaction Engineering of Step Growth Polymerization,* Plenum, New York, 1987.
15. S. K. Gupta, *Numerical Methods for Engineers,* Wiley Eastern, New Delhi, 1994.
16. G. S. G. Beveridge and R. S. Schechter, *Optimization: Theory and Practice,* McGraw-Hill, New York, 1970.
17. V. Chankong and Y. Y. Haimes, *Multiobjective Decision Making—Theory and Methodology,* Elsevier, New York, 1983.

Received December 1, 1994
Accepted January 8, 1995